SolarPACES 2024, 30th International Conference on Concentrating Solar Power, Thermal, and Chemical Energy Systems

Solar Collector Systems

https://doi.org/10.52825/solarpaces.v3i.2365

Published: 26 Jan. 2026

Modeling and Energetic Analysis of a Supercritical Carbon Dioxide sCO_2 Recompression-Organic Rankine Cycle Integrated to a Central Tower Receiver.

J.A. Moctezuma-Hernandez[1,*], Judit García-Ferrero[1], Rosa P. Merchan[1], J.M. Belman-Flores[2], Sergio Cano-Andrade[2], and J.M.M Roco[1]

[1]Department of Applied Physics, Universidad de Salamanca, Salamanca, Spain.

[2]Department of Mechanical Engineering, Universidad de Guanajuato, Salamanca, GTO 36885, México.

*Correspondence: J.A Moctezuma-Hernandez, ja.moctezuma@usal.es

Abstract. This study presents a comprehensive thermodynamic model and energetic analysis of a hybrid Concentrated Solar Power (CSP) system incorporating a supercritical carbon dioxide (sCO_2) Brayton cycle and an Organic Rankine Cycle (ORC). The CSP system uses a central tower receiver with a fluidized particle-in-tube of silicon carbide particles and air as the heat transfer medium. Operating at a temperature of 650 °C, the system demonstrates a heat transfer coefficient of 411 W/m^2K. Key findings highlight the sensitivity of the convective coefficient to gas velocity and the effect of particle mass flow on receiver efficiency. Fuel mass flow reductions of up to 3.7% were achieved through particle mass flow adjustments, while variations in compression ratio and vapor turbine inlet temperature affected overall cycle performance and efficiency. The study highlights the potential of such integrated systems to improve thermal efficiency, although further optimization is needed to balance fuel consumption and environmental impact.

Keywords: Concentrated Solar Power, Fluidized Bed, Supercritical CO_2, ORC

1. Introduction.

The use of solar energy for power generation has gained significant importance due to its renewable nature and its potential to reduce carbon emissions. In this sense, in the last decades there has been a growing interest in Concentrating Solar Power (CSP) plants, especially in solar power towers, where the solar radiation captured by a heliostat field is concentrated in a receiver, which can be a particle receiver. Inside this solar receiver, a heat transfer fluid is used to raise its temperature to values above 500 °C [1]. This heat transfer fluid can be integrated into a power system, either a Rankine cycle or a Recompression Brayton cycle, for electrical power generation. The use of a fluidized bed of air and solid particles as a heat transfer fluid has been shown to be a promising way to improve energy capture from solar radiation. An effective heat transfer fluid within the particle receiver is key to achieving high temperatures. In this line, Perez-Lopez *et al.* [2] experimented with a solar receiver with a Dense Particle Suspension (DPS), where the particles were silicon carbide (SiC) with a volume fraction of 30%. Sixteen tubes were used. The tests were performed with a mass flow variation of 660-1760 $\mathrm{kg/h}$ and a solar thermal power of 60-142 kW. The results showed a DPS outlet

temperature of 700°C and receiver efficiencies between 50% and 90%. Another important advantage of using a dense particulate or fluidized bed solution over other heat transfer fluids, such as molten salts, is the cost of operation and maintenance. On the other hand, in recent years, Brayton cycles with supercritical carbon dioxide (sCO_2) have attracted great interest in their coupling with concentrating solar power plants because they have proven to be more compact, safer, and economically more profitable [3], [4]. Another positive aspect of using CO_2 is that its critical pressure is low (7.37 MPa), in addition to being non-toxic and non-flammable [5]. When CO_2 is operated at conditions very close to its critical point, it becomes very dense, requiring very little compression work. The low compression work and high temperatures in the cycle result in higher thermodynamic efficiencies than in a conventional Rankine cycle [6]. In addition, Brayton recompression cycles show the best energy performance compared to other configurations [7]. In this sense, Wu *et al.* [8] performed an "exergo-economic" analysis of a supercritical carbon dioxide recompression Brayton cycle coupled to an organic flash cycle. These results show the effectiveness of this type of cycle and the improvement in energy efficiency. Organic Rankine cycles (ORC) are also cycles that have been used to convert low temperature waste heat into electrical energy. Unlike the conventional Rankine cycle that uses water, these systems use organic fluids that have favorable thermodynamic properties and allow them to operate at lower temperatures.

This work presents an analysis of a power system consisting of a recompression Brayton cycle with $\mathrm{sCO_2}$ and an organic Rankine cycle utilizing refrigerant R152a as the working fluid. The power system is coupled to a concentrating solar power plant, specifically to a central receiver, utilizing a fluid of particles and air as the heat transfer system. The particle receiver is modeled with the objective of first understanding and then reproducing the heat transfer process. The fluidized bed, comprising a combination of silicon carbide particles and air, serves as the heat transfer fluid. The outlet temperature of the particle receiver is set at 650 °C. Subsequently, a parametric analysis of the particle receiver is conducted, examining the effects of varying the gas velocity, the volume fraction of particles in the suspension, the tube diameter, and the thermal efficiency of the receiver. Furthermore, the impact of these parameters on the energy performance of the Brayton cycle, as well as the power and mass flow of the fuel, is examined.

2. Modeling

The modeling of the particle receiver system and heat transfer between the heliostat field radiation and the fluidized bed presented in this work is based on the works done by Gallo *et al*. [9] and Córcoles *et al*. [10], respectively. On the other hand, the modeling of the power cycle performance is described by energy and mass balances in each component. The software used to model the system is Mathematica [11].

2.1 Particle Receiver

A mixture of two fluids, silicon carbide and air, circulates inside the particle receiver. The calculation of the thermodynamic properties of this fluid mixture (fluidized bed) is presented below. In [12] some values of the properties of silicon carbide are given. All thermodynamic properties were evaluated using the mean temperature. In Eqs (1)-(3), the mass flow per unit area of the fluidized bed (G_{DPS}) and specific heat of the fluidized bed $(C_{p,DPS})$, are calculated [9].

$$G_{DPS} = \varphi_p \rho_p \left(u_g - u_{mf}\right) + (1 - \varphi_p)\rho_g u_g \tag{1}$$

$$\rho_{DPS} = \varphi_p \rho_p + (1 - \varphi_p)\rho_g \tag{2}$$

$$C_{p,DPS} = \frac{\varphi_p \rho_p C_{p,p} + (1-\rho_p)\rho_g C_{p,g}}{\varphi_p \rho_p + (1-\varphi_p)\rho_g} \quad (3)$$

These equations are expressed in terms of the volumetric fraction of particle suspension, φ_p; the gas velocity, u_g; the minimum fluidization velocity, u_{mf}; and the specific heat of the particle and gas $C_{p,p}, C_{p,g}$, respectively. Once the thermodynamic properties are known, the mass flow rate of the fluidized bed $(\dot{m}_{DPS})$ can be calculated. This flow rate is the sum of the particle and gas mass flow rates, $(\dot{m}_p, \dot{m}_g$, respectively). By performing an energy balance inside the particle receiver, these variables can be calculated as seen in Eqs. (4) and (5), where $\dot{Q}_{rec}$ is the thermal power delivered to the receiver by the heliostat field, in this work $\dot{Q}_{rec} = 57\ MW$ [9]. The $\dot{Q}_{losses}$ are calculated considering the heat losses by radiation and convection from the tube to the environment. Calculated heat losses $\dot{Q}_{rec}$ is updated. The outlet temperature of the particle receiver is set to $T_p^{out} = 650\ °C$. This analysis was performed iteratively, since the inlet temperature of the particles in the receiver (T_p^{in}) is proposed at the beginning of the calculation. The convergence criterion is to analyze the thermodynamic properties of the past iteration with the current one, if the difference is less than 0.01 the iterative process ends. This process can be seen in Caption 1.

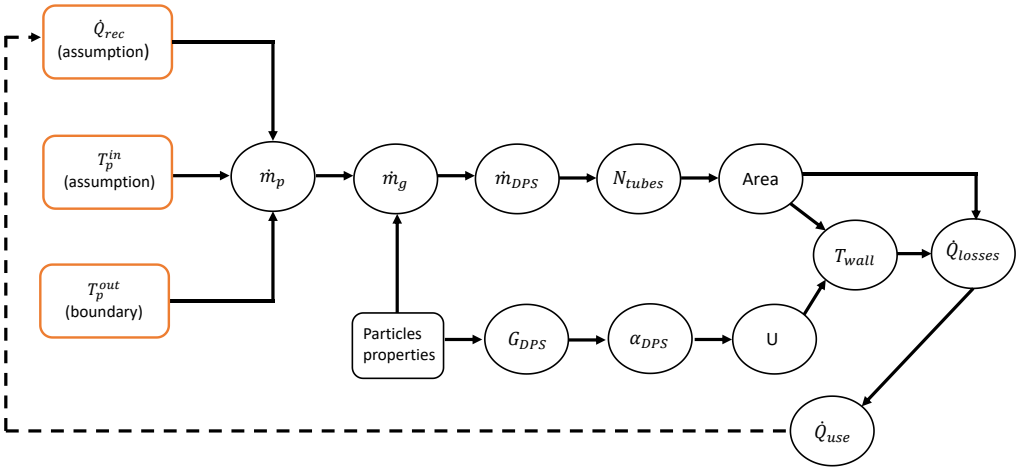

Figure 1. *Iterative process for particle receiver modeling.*

$$\dot{m}_p = \frac{\dot{Q}_{rec}}{C_{p,p}(T_p^{out} - T_p^{in})} \quad (4)$$

$$\dot{m}_g = \frac{(1-\varphi_p)\rho_p u_g}{\varphi_p \rho_p (u_g - u_{mf})} \dot{m}_p \quad (5)$$

Then, the calculation of the number of tubes (N_{tubes}) needed to reach the set temperature at the outlet of the receiver is $N_{tubes} = \frac{4\dot{m}_{DPS}}{\pi d_i^2 G_{DPS}}$, where d_i is the internal diameter of the tube. Developing a model that describes the heat transfer process inside the particle receiver is complex. The energy transfer process begins when solar radiation from the heliostat field hits the tubes. This radiation heats the tube wall and raises its temperature, which in turn allows convection and conduction to heat the fluidized bed, whose particles gain a higher temperature. This energy transfer process is shown graphically in Figure 2.

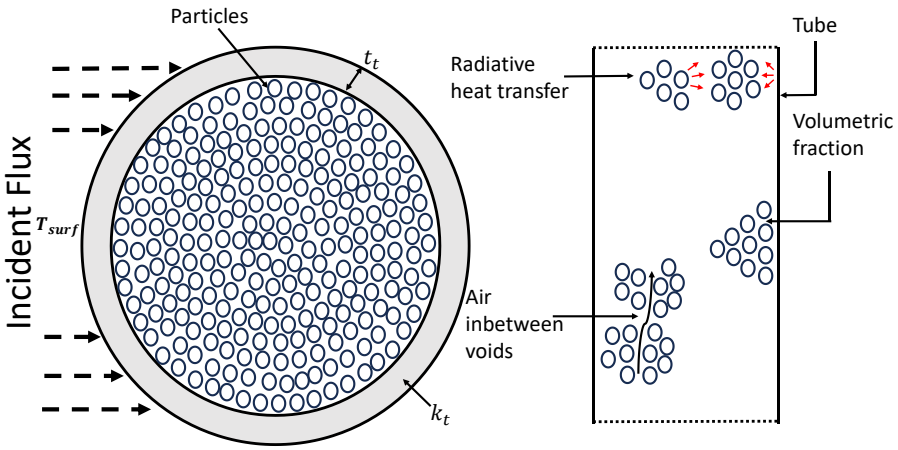

Figure 2. *Heat transfer process inside the receiver.*

This whole process of energy transfer is described through the global coefficient of heat transfer (U), which is in Eq. (6). This equation is obtained from the analysis of the global coefficient for cylindrical coordinates. f_{act} is the active front fraction of the tube, which only considers the part where the solar radiation is impacting the tube, as shown in Caption 2. t_t is the thickness of the tube, k_t is the thermal conductivity of the tube α_{DPS} is the convective heat transfer coefficient. This last coefficient is of special interest because it is responsible for modeling the energy transfer inside the particle receiver. To obtain the convective coefficient of the fluidized bed, the correlations used come from the work developed by Gallo et al. [9]. This analysis can be performed in an empirical or semi-empirical manner. In this work semi-empirical correlations were used. Eq. (7) allows the evaluation of the heat transfer coefficient and involves the convective coefficient (α_{DPS}), which contributes 70% to the total heat transfer coefficient [13]. Full details of Eqs (9)-(13) can be found in Corcoles et al. [10].

$$U = f_{act}\alpha_{DPS} + 2\frac{\sqrt{\alpha_{DPS}k_t t_t}}{\pi d_i} tanh\left[\pi\left(d_i + \frac{t_t}{2}\right)\left(\frac{1-f_{act}}{2}\right)\sqrt{\frac{\alpha_{DPS}}{k_t t_t}}\right] \tag{6}$$

$$\alpha_{DPS} = 0.7\alpha_w + \alpha_{rad} \tag{7}$$

$$\alpha_{rad} = 7.3(\epsilon_p \epsilon_t \sigma T_{mean}^3) \tag{8}$$

$$\alpha_w = \alpha_g + f_p\alpha_p + \alpha_{gp} \tag{9}$$

$$f_p = 1 - e^{-10\left(\frac{\varphi_p}{\varphi_{cp}}\right)} \tag{10}$$

$$\alpha_g = (c_0 Re_L^{n1} Pr^{n2} + c_1)\frac{k_g}{L} + c_2 \tag{11}$$

$$\alpha_p = (c_3 Re_p^{n3})\frac{k_g}{d_p} \tag{12}$$

$$\alpha_{gp} = \left(c_4 Re_p^{n4} Pr_r^{n5} + c_5\right)\frac{k_g}{d_p} + c_6 \tag{13}$$

The evaluation of α_{DPS} from Eq. (7) in turn, requires the evaluation of α_w, which can be performed by using the semi-empirical correlations and is calculated by the Eqs. (9)-(13). Once the heat transfer process is described, the temperature at the wall of the tube, $Twall$, can be calculated, assuming that the tube has a constant heat flow and using Newton's law of cooling equation [14], in which the heat flow is considered to not impact the entire circum-ference of

the tube. This process is described in Capture 3. Care must be taken to avoid reaching the melting temperature of the material, which is 1127–1187 K for AISI 310S stainless steel [15]. In addition, convective and radiative heat loss can be calculated by using Eq. (15) and (16). Finally, using Eq. (17), the process is fed back with the obtained value of $\dot{Q}_{use}$, allowing the iterative cycle shown in Caption 1 to be completed once the inlet temperature of the particles is recalculated using Eq. (4).

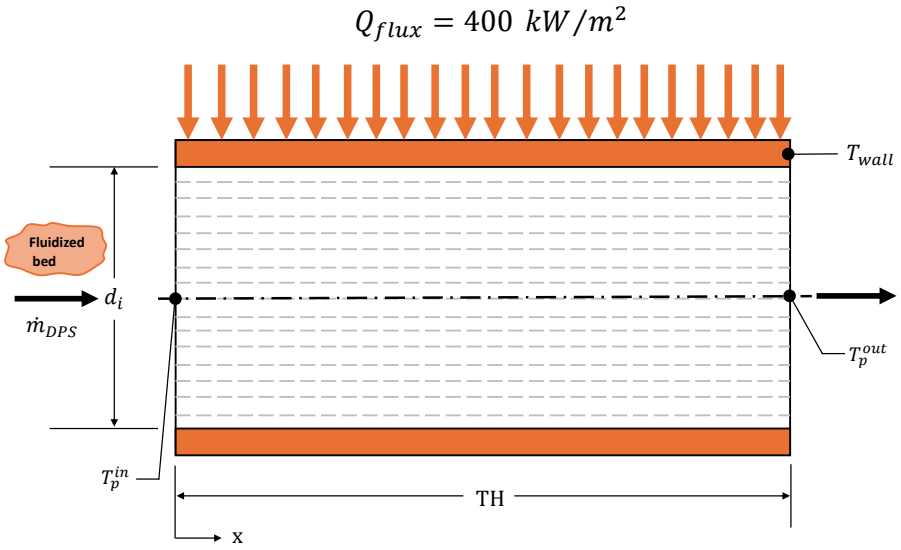

Figure 3. *Calculation of tube wall temperature.*

$$\dot{Q}_{losses} = \dot{Q}_{conv} + \dot{Q}_{rad} \tag{14}$$

$$\dot{Q}_{conv} = (1 - f_{act})\alpha_{DPS} A_{tubes}(T_{wall} - T_a) \tag{15}$$

$$\dot{Q}_{rad} = (1 - f_{act})\epsilon_t \sigma A_{tubes}(T_{wall}^4 - T_a^4) \tag{16}$$

$$\dot{Q}_{use} = \dot{Q}_{rec} - \dot{Q}_{losses} \tag{17}$$

2.2 Performance criteria

The thermal efficiency of the particle receiver, η_{threc}, is used to evaluate the performance of the system. It is defined from Eq. (18) as the actual heat absorbed by the fluidized bed divided by the ideal heat that could be absorbed. The evaluation of the actual heat depends on convective and radiative heat losses, see Eqs. (14) and (17), as well as on the power supplied to the compressor and the mechanism to move the particles. Finally, the energy consumed by the compressor to move the air, $\dot{E}_{comp}$, and the energy required by the mechanism to transport the particles to the receiver, $\dot{E}_{scew}$, are obtained from Eqs. (20) and (21), where η_{mec} and η_p represent the mechanical and polytropic effi-ciencies, respectively. For this analysis, η_{mec}=0.8 and η_p=0.98 [15]. In Eq. (22) [9] the necessary pressure in the fluidized bed is calculated for the system to work properly.

$$\eta_{threc} = \dot{Q}_{total} \Big/ \dot{Q}_{rec} \tag{18}$$

$$\dot{Q}_{total} = \dot{Q}_{use} - \dot{E}_{screw} - \dot{E}_{comp} \tag{19}$$

$$\dot{E}_{screw} = \frac{\dot{m}_p(P_{base} - P_a)}{\eta_{mec} f_p \rho_p} \tag{20}$$

$$\dot{E}_{comp} = \frac{\dot{m}_g C_{p,g} T_a}{\eta_{mec}} \left[\left(\frac{P_{base}}{P_a} \right)^{\frac{r_g}{\eta_p C_{p,g}}} - 1 \right] \tag{21}$$

$$P_{base} = P_a + g\rho_{DPS} TH + 0.184 \left(\frac{G_{DPS} d_i}{\mu_{DPS}} \right)^{-0.2} \frac{TH}{d_i} \frac{G_{DPS}^2}{2\rho_{DPS}} \tag{22}$$

2.3 Power block

Once the heat transfer analysis of the solar receiver is complete, the power cycle analysis can be performed. Caption 4 shows the schematic of the power cycle coupled to the particle receiver. The power cycle consists of a Brayton recompression cycle with supercritical carbon dioxide (sCO_2) coupled to an Organic Rankine Cycle (ORC). The input data for each cycle can be seen in Table 1. The analysis of the cycle is performed by means of a mass and energy balance, as seen in the following subsection. The choice of this layout is supported by the results obtained by Akbari *et al*. [16] for the sCO_2 power Brayton cycle, and the refrigerant in the ORC.

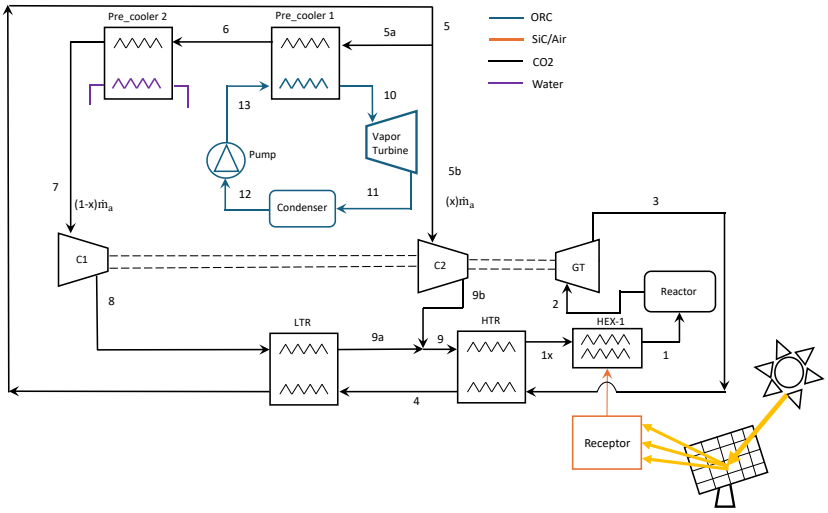

Figure 4. *Diagram of the supercritical Brayton cycle coupled to the particle receiver and the organic Rankine cycle.*

Table 1. *Input data for sCO2RBC and ORC simulation.*

Subsystem	Parameters	Value
sCO2 recompression Brayton Cycle (sCO2RBC)	p_2 (bar)	74
	$\dot{m}_a$ (kg/s)	2943
	r_p	3
	η_c	0.85
	$\dot{Q}_{LHV}$ (kW)	47141
Organic Rankine Cycle (ORC)	T_{10} (K)	360
	p_{10} (bar)	5.37
	$\epsilon_{Pre\_cooler1}$	0.86
	$\dot{m}_o$ (kg/s)	450.5
	η_{pump}	0.8

2.3.1 Power Cycle Model (Brayton Cycle)

By performing a mass and energy balance in each component, it is possible to know the temperatures, heat and work [17], as shown in equations (23) and (24). For the heat exchangers, efficiency has been considered to have the following values: effectiveness of the recuperator (ϵ_{HTR}) of 0.86, effectiveness of the solar receiver (ϵ_{HS}) of 0.9, of the combustion (ϵ_{HC}) of 0.85.

$$\sum \dot{m}_{in} = \sum \dot{m}_{out} \tag{23}$$

$$\sum \dot{Q} + \sum \dot{m}_{in} h_{in} = \sum \dot{W} + \sum \dot{m}_{out} h_{out} \tag{24}$$

There is a special analysis for the processes occurring inside the reactor, where the equation is the following, $|\dot{Q}_{HC}| = \epsilon_{HC} |\dot{Q}_{1-2}| = \epsilon_{HC} \eta_c \dot{m}_f Q_{LHV}$. Where η_c is the combustion efficiency, $\dot{m}_f$ is the mass flow of the fuel and Q_{LHV} is the low heating value of the fuel [18]. The total heat contributed to the cycle is the sum of the heat contributed by the recuperator and the heat contributed by combustion ($\dot{Q}_h = \dot{Q}_{HS} + \dot{Q}_{HC}$). The same type of analysis is applied to the ORC cycle, and equations (23) and (24) are used to evaluate each of the components.

3. Validation of the particle receiver model

The geometric and heat transfer data of the particle receiver are compared with values reported in the literature. The study by Belmonte *et al*. [12] was used as a reference, as it employs the same geometrical analysis previously conducted by Gallo *et al*. [9]. The comparison was made with the convective heat transfer coefficient, which had a relative error of 4.4% when comparing the model of the current work with the literature. The particle mass flow had a relative error of 3.3% and the number of tubes was 2%. This maximum relative error of 11% corresponds to the calculation of the absorption area, where the error propagates, resulting in the highest error among the analyzed variables. Nevertheless, the behavior of the particle receiver model shows a good performance.

4. Results

The results of the parametric analysis are shown in Caption 5. Caption 5a shows that the thermal efficiency of the receiver increases as the diameter of the tubes increases. It should be noted that not all the diameters shown in this graph can be used. Nevertheless, the volume fraction of the particles in suspension is varied to observe the behavior of the system, since it has been noticed that this variable is very important for the correct operation of the particle receiver. As the diameter of the tube and the volume fraction of the particles decrease, the efficiency of the particle receiver decreases. On the other hand, in Caption 5b, the total heat transfer area is very sensitive to the gas velocity. If the gas velocity is increased from 0.12 to 0.16, the absorption area decreases by 25%. Another interesting value is the volume fraction of the particles, because if it decreases, the absorption area increases significantly. This is because the volume fraction of particles is directly proportional to the mass flow per unit area (see Eq. 1), which is inversely proportional to the number of tubes. In Caption 5c, the heat transfer coefficient is varied against the gas velocity, and it is seen that the convective coefficient is very sensitive to the gas velocity while the mass flow of particles inside the receiver is also varied. It is observed that as the mass flow decreases, the convective coefficient increases. One would think that it is better to work with a smaller number of particles in the receiver, but Caption 5d shows that as the volume fraction of these particles decreases, there is a point at which the energy efficiency of the receiver becomes zero. Therefore, a balance between particle mass flow rate, gas velocity, and tube diameter must be achieved to reach adequate receiver energy efficiency.

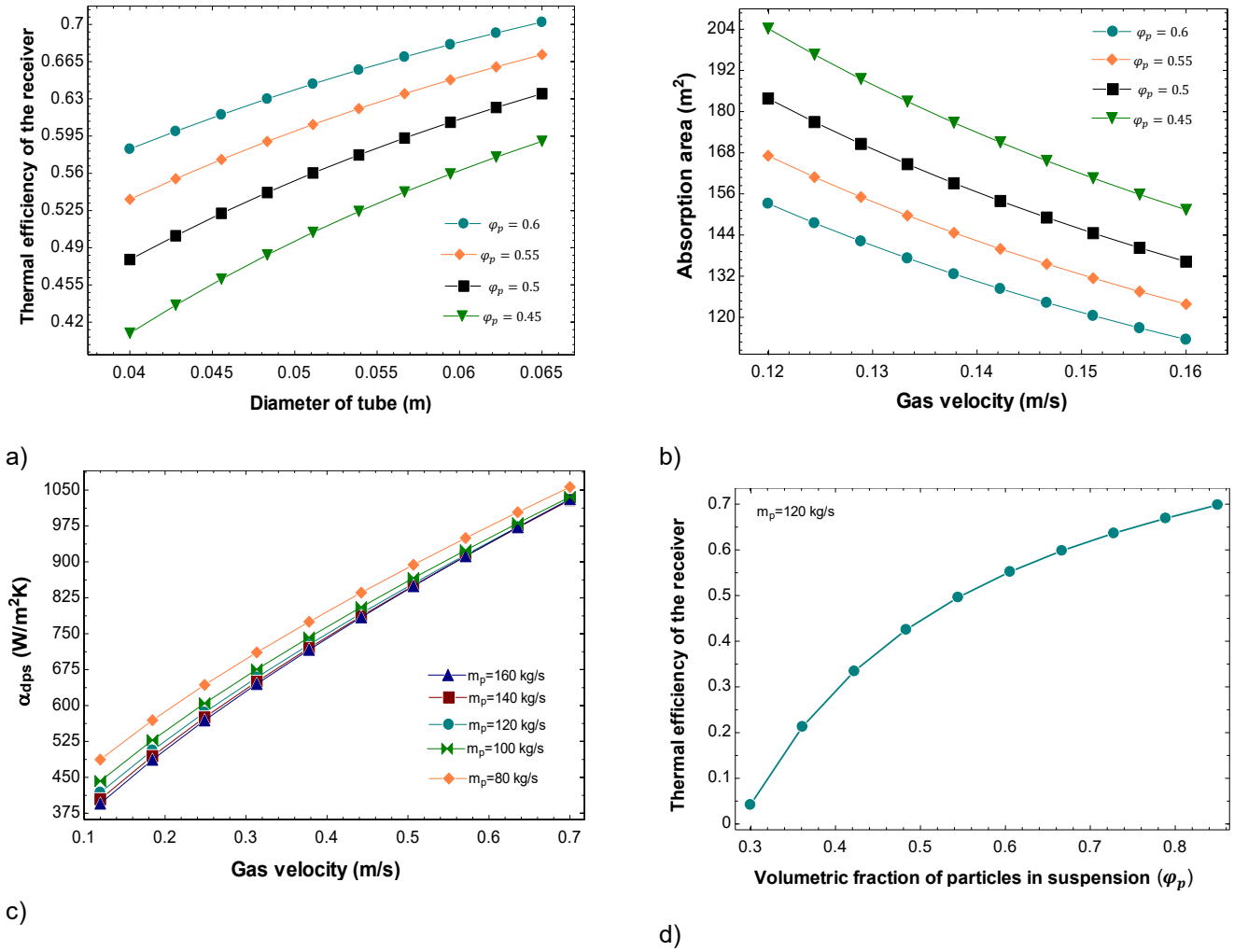

Figure 5. *Parametric analysis of the particle receiver. a) Variation of the efficiency of the particle receiver at different pipe diameters and varying the volumetric fraction of the particles in the system. b) Absorption area of the receiver versus gas velocity varying the volumetric fraction of the particles. c) Convective heat transfer coefficient in the receiver versus gas velocity varying the mass flow of the particles. d) Thermal efficiency of the receiver versus the volumetric fraction of the particles.*

As can be seen in Caption 6a, the interaction of the particulate receiver with the power cycle fuel mass flow has minimal effect on the increase or decrease of the particulate mass flow in the solar receiver for fuel consumption. This is mainly due to the high CO_2 mass flow in the Brayton cycle, which does not affect the fuel consumption too much. However, Caption 6b analyzes the total power variation of the Brayton-ORC cycle. With a compression ratio of the Brayton cycle of 4, a total net power of 385 MW can be achieved and a vapor turbine inlet temperature (T_{10}) of 330 K. As the steam turbine inlet temperature increases, the temperature at the inlet of Compressor 1 (C1) increases, resulting in higher energy consumption, lower net power, and lower overall thermal efficiency, as shown in Caption 6c. Compression ratio is an important element in the power cycle. In FCaption 6b and 6c, a variation from 2.2 to 4 is observed, and the increase in total power and efficiency is 77.9% and 77.7%, respectively.

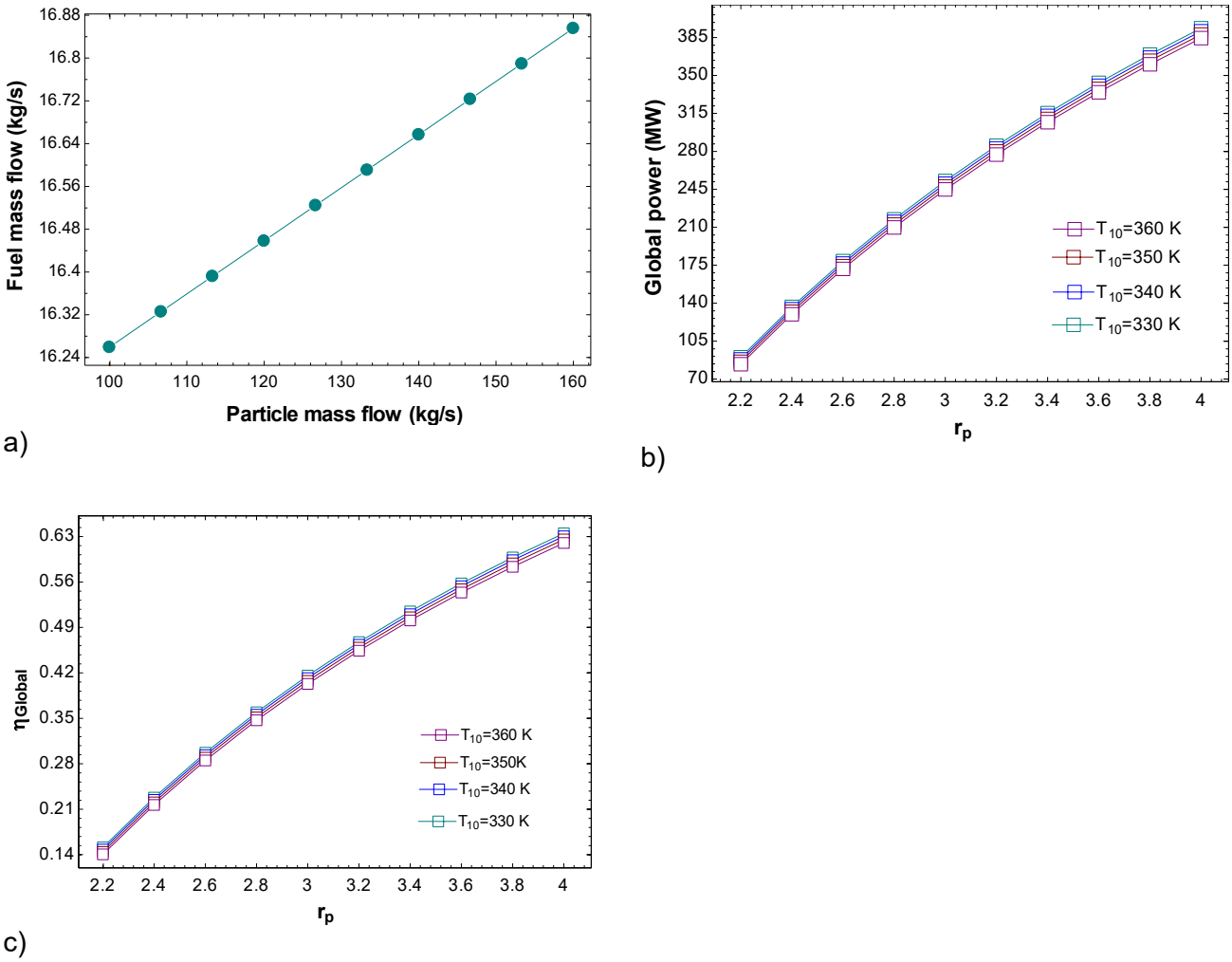

Figure 6. *a) Mass flow variation of the power cycle fuel concerning the mass flow of the particles inside the solar receiver. b) variation of the overall cycle power concerning the compression ratio and varying different inlet temperatures to the organic cycle turbine. c) Variation of the overall efficiency concerning the compression ratio with different temperatures in the steam turbine.*

5. Conclusions

In this work, the analysis of a fluidized bed particle receiver coupled to a supercritical CO_2 Brayton cycle and an organic Rankine cycle was performed. The parametric analysis within the particle receiver yielded significant results. The high sensitivity of the convective coefficient to the gas velocity was observed. The particle mass flow and the particle volumetric fraction play an important role in this receiver, because when the particle mass flow is reduced, the convective coefficient improves its performance, but the particle volume fraction cannot be drastically reduced, since there is a point where the thermal efficiency of the receiver can be zero. Nevertheless, coupling the solar receiver to the power cycle shows that a fuel mass flow reduction of up to 3.7% can be achieved by varying the receiver particle mass flow. The total power and efficiency of the cycle are analyzed as a function of the compression ratio. The sensitivity of these two variables to the compression ratio is shown. The inlet temperature of the vapor turbine is also analyzed, and it is observed that as this temperature increases, the overall efficiency and power decrease. Finally, there is a need for further analysis of this type of fluidized particle-in-tube solar receiver to observe the most appropriate configuration for better energy performance. The power cycle analyzed shows a high overall thermal efficiency and power, as well as a high fuel consumption, which indicates that further work is needed to

optimize these electrical energy production systems and, in turn, make them more environmentally friendly.

Data availability statement

No additional materials (e.g., source code, simulation data, or videos) have been deposited in a public repository. The Mathematica modeling code and the datasets used to generate the results presented in this article are available from the corresponding author upon reasonable request (**ja.moctezuma@usal.es**).

Underlying and related material

The detailed modeling of the solar central-tower particle receiver (Mathematica and EES scripts) is published in:

Moctezuma-Hernandez J.A., Merchán R.P., Roco J.M.M., "Supercritical CO_2 hybrid Brayton–Organic Rankine Cycle integrated with a solar central tower particle receiver: Performance, exergy analysis, and choice of the organic refrigerant," Renewable Energy 250 (2025) 123231. DOI: **https://doi.org/10.1016/j.renene.2025.123231**.

No further supplementary code or datasets have been deposited in a public repository; these materials are available from the corresponding author upon reasonable request (**ja.moctezuma@usal.es**).

Author contributions

J.A. Moctezuma-Hernandez: Conceptualization, Methodology, Software, Formal analysis, Data curation, Writing—Original Draft, Visualization.

Judit García-Ferrero: Methodology, Investigation, Writing—Review & Editing.

Rosa P. Merchán: Methodology, Investigation, Writing—Review & Editing.

J.M. Belman-Flores: Writing—Review & Editing.

Sergio Cano-Andrade: Writing—Review & Editing.

J.M.M. Roco: Conceptualization, Supervision, Formal analysis, Funding acquisition, Project administration, Writing—Review & Editing.

Competing interests

The authors declare that they have no competing interests.

Funding

J.A.Moctezuma-Hernandez acknowledges financial support from CONACYT-México CVU 1006749. The authors acknowledge Universidad de Salamanca and funding from Ministerio de Ciencia, Innovación y Universidades of Spain under grant PID2023-147201OB-I00.

Acknowledgement

The authors would like to thank the research group “Optimización Energética, Termodinámica y Física Estadística” of the University of Salamanca for their invaluable support and insightful discussions throughout this work.

References

[1] Flamant, G., Gauthier, D., Benoit, H., Sans, J. L., Garcia, R., Boissière, B., ... & Hemati, M. (2013). Dense suspension of solid particles as a new heat transfer fluid for concentrated solar thermal plants: On-sun proof of concept. *Chemical engineering science*, *102*, 567-576, doi: https://doi.org/10.1016/j.ces.2013.08.051.

[2] Lopez, I. P., Benoit, H., Gauthier, D., Sans, J. L., Guillot, E., Mazza, G., & Flamant, G. (2016). On-sun operation of a 150 kWth pilot solar receiver using dense particle suspension as heat transfer fluid. *Solar Energy*, *137*, 463-476, doi: https://doi.org/10.1016/j.solener.2016.08.034

[3] Hay, R., & Celik, K. (2020). Accelerated carbonation of reactive magnesium oxide cement (RMC)-based composite with supercritical carbon dioxide (scCO2). *Journal of Cleaner Production*, *248*, 119282, doi: https://doi.org/10.1016/j.jclepro.2019.119282.

[4] Sharan, P., Neises, T., & Turchi, C. (2018). Optimal feed flow sequence for multi-effect distillation system integrated with supercritical carbon dioxide Brayton cycle for seawater desalination. *Journal of Cleaner Production*, *196*, 889-901, doi: https://doi.org/10.1016/j.jclepro.2018.06.009.

[5] Liu, Z., Cao, X., Wang, T., Jia, W., & Duan, Z. (2019). Comparative evaluation of the refrigeration compressor performance under different valve parameters in a trans-critical CO2 cycle. *International Journal of Refrigeration*, *101*, 34-46, doi: https://doi.org/10.1016/j.ijrefrig.2019.02.034.

[6] Ahn, Y., Bae, S. J., Kim, M., Cho, S. K., Baik, S., Lee, J. I., & Cha, J. E. (2015). Review of supercritical CO2 power cycle technology and current status of research and development. *Nuclear engineering and technology*, *47*(6), 647-661, doi: https://doi.org/10.1016/j.net.2015.06.009.

[7] Padilla, R. V., Too, Y. C. S., Benito, R., & Stein, W. (2015). Exergetic analysis of supercritical CO2 Brayton cycles integrated with solar central receivers. *Applied Energy*, *148*, 348-365, doi: https://doi.org/10.1016/j.apenergy.2015.03.090.

[8] Wu, C., Wang, S. S., & Li, J. (2018). Exergoeconomic analysis and optimization of a combined supercritical carbon dioxide recompression Brayton/organic flash cycle for nuclear power plants. *Energy Conversion and Management*, *171*, 936-952, doi: https://doi.org/10.1016/j.enconman.2018.06.041.

[9] Gallo, A., Spelling, J., Romero, M., & González-Aguilar, J. (2015). Preliminary design and performance analysis of a multi-megawatt scale dense particle suspension receiver. *Energy Procedia*, *69*, 388-397, doi: https://doi.org/10.1016/j.egypro.2015.03.045.

[10] Córcoles, J. I., Díaz-Heras, M., Fernández-Torrijos, M., & Almendros-Ibáñez, J. A. (2023). Flow and heat transfer analysis of a gas–particle fluidized dense suspension in a tube for CSP applications. *Renewable Energy*, *206*, 1-12, doi: https://doi.org/10.1016/j.renene.2023.02.004.

[11] Inc. Wolfram Research, “Mathematica, Version 13.2.” Champaign, IL, 2023.

[12] Reyes-Belmonte, M. A., Sebastián, A., Spelling, J., Romero, M., & González-Aguilar, J. (2019). Annual performance of subcritical Rankine cycle coupled to an innovative particle receiver solar power plant. *Renewable energy*, *130*, 786-795, doi: https://doi.org/10.1016/j.renene.2018.06.109.

[13] Molerus, O., & Wirth, K. E. (2012). *Heat transfer in fluidized beds* (Vol. 11). Springer Science & Business Media, doi: 10.1007/978-94-011-5842-8.

[14] Collings, E. W., Jelinek, F. J., Ho, J. C., & Mathur, M. P. (1977). Magnetic and thermal properties of stainless steel and Inconel at cryogenic temperatures. In *Advances in Cryogenic Engineering: Volume 22* (pp. 159-173). Boston, MA: Springer US.

[15] Spelling, J., Gallo, A., Romero, M., & González-Aguilar, J. (2015). A high-efficiency solar thermal power plant using a dense particle suspension as the heat transfer fluid. *Energy Procedia*, *69*, 1160-1170.

[16]Akbari, A. D., & Mahmoudi, S. M. (2014). Thermoeconomic analysis & optimization of the combined supercritical CO2 (carbon dioxide) recompression Brayton/organic Rankine cycle. *Energy*, *78*, 501-512, doi: https://doi.org/10.1016/j.energy.2014.10.037.

[17]Bergman, T. L., Lavine, A. S., Incropera, F. P., & DeWitt, D. P. (2011). *Introduction to heat transfer*. John Wiley & Sons.

[18]Olivenza-León, D., Medina, A., & Hernández, A. C. (2015). Thermodynamic modeling of a hybrid solar gas-turbine power plant. *Energy Conversion and Management*, *93*, 435-447, doi: https://doi.org/10.1016/j.enconman.2015.01.027.